Effectiveness of Nonlinear Modelling and Computer Aided Design based Technique in the Control System

Imran S. Sarwar

Abstract— Two methods for modeling of mechatronics system such as pan tilt platform (PTP) are presented based on Lagrange-Euler (LE) modeling method and Computer Aided Design (CAD) based technique. The objective of this research work is to derive nonlinear model of PTP, apply the controller for motion control of PTP, check the stability and create virtual simulation of the PTP to point in a desired direction. To increase the number of matching parameters and to preserve the structural properties and apply non-rigid body effects of PTP, in the second approach the virtual simulation of PTP is developed using CAD based technique. The LE model with Proportional-Derivative (PD) controller and virtual simulation gave us desired orientation of camera with slight difference in their settling time and steady-state error. This is due to the effect of backlash, saturation and dead zone as they are present in the virtual simulation. They meet the desired performance values set according to movement of eye ball such as settling time of eye ball is approximately 0.18~0.22 seconds.

Index Terms— CAD based technique, control system, identification of parameters, Implementation, kinematics, Lagrange-Euler, robotics, simulation, security systems.

1 Introduction

THE PTP, with two degrees of freedom, is a device that makes possible for the camera to point in a desired direction. The computer aided design (CAD) as shown in Fig. 1 (b) has been used in the virtual simulation software in Section VI. In the virtual simulation, constraints were applied on each joint. The types of joints are rigid, revolute and motorized. The CAD based simulation was performed in the presence of backlash, dead zone, friction and gravity. In designing the system, we also took care of the singularity that may arise when the system Jacobian approaches zero [4]-[6]. The forward kinematics of the PTP are developed using Euler rotation theorem from [1]. The inverse kinematics of the PTP is developed using Paul's method [17].

The system modeling of a mechatronic system such as the PTP generally involves complex physical realities, which are usually simplified to build the system model. The linear model does not include the preliminary nature of nonlinearities [12]. The linear system model in [2] has oscillations that are only possible for differential equations with purely imaginary eigenvalues for example a system marginally stable has poles on imaginary axis. The negative real parts lead to damped oscillations. The inclusion of nonlinearities allows us to achieve accurate model of PTP.

The behavior of the PTP is highly sensitive to system parameters. The small variations in the PTP parameters have either ended the oscillations or driven the system into random operation [9]. Therefore, we have built non-linear model of the PTP using [2]. The viscous friction, Coulomb friction, mass and inertia have been identified and these values are used in the simulations. The parameters friction, Coriolis forces and backlash were calculated. Mass properties are obtained from CAD for modeling and simulation purposes.

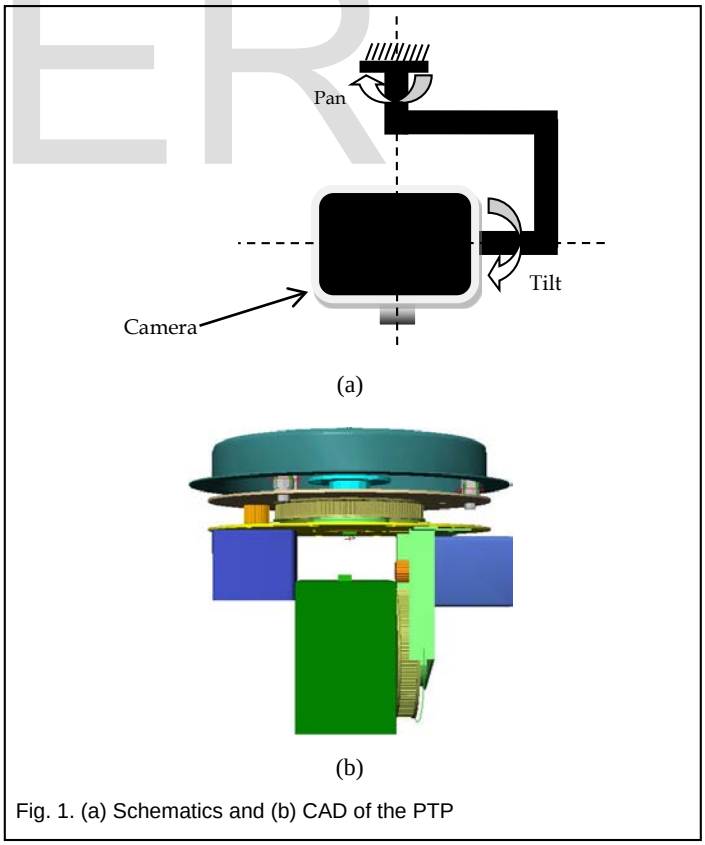

Fig. 1. (a) Schematics and (b) CAD of the PTP

The LE model and virtual simulation are presented in Sections V and VI respectively. To perform the analysis and simulation requires the parametric identification. All the parameters

• *Imran S. Sarwar is working as a lecturer in the Air university, Pakistan PH-00923419507775; email: imransarwar@mail.au.edu.pk.*

involved in system dynamics were identified. The PD controllers have been applied to the PTP for both axes, and the desired results were achieved. The industry increasingly relies on the use of computer simulation technology to reduce the number of hardware tests required. This can be done by the object-oriented simulation environment. A physical model of the PTP is presented and transformed into a dynamical simulation model. The purpose behind this was to generate a virtual simulation of the physical model. This approach was tested and compared with the nonlinear model of the PTP to prove the effectiveness of the method.

For the validation of results we have used professional simulation software packages that consist of Pro-Engineer (Pro-E), MSC VisualNastrn-4D and MATLAB/Simulink. The three software can be connected together and enable us to establish a simulation environment as shown in Fig. 2. Each of the software can handle the following items.

- Pro-Engineer: For modeling and assembling the mechanical components.
- VisualNastran-4D: For simulation of static and dynamic behavior of the mechanical system.
- MATLAB/Simulink: For the motion control of the mechanical system in VisualNastran-4D.

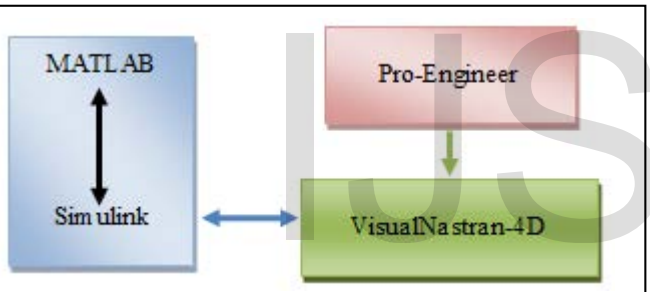

Fig. 2. The software connectivity diagram

Already published papers in this field are not sufficient for a mechatronic system. Mostly papers published have discussed but not applied the virtual simulation on mechatronic systems. [19]

The system model of the PTP is developed in Section II and the system model of the PTP along with the PD controllers is presented in Section V. The system parameters were identified and given in tabulated form in Section III. The CAD model of the PTP with the PD controllers is presented in Section VI. The PD controllers have been derived from a linear system model already reported [12], and is being applied to control the motion of the PTP.

2 System Model

The basis for the model of the PTP is LE equation from [1]-[3]. The PTP is a two link robot. The nonlinear dynamic equations for a 2-link robot take the form as:

$$\tau = M(\theta)\ddot{\theta} + C(\theta,\dot{\theta})\dot{\theta} + F_v\dot{\theta} + F_c\, sgn(\dot{\theta}) + g(\theta) \quad (1)$$

τ (torque) is control input and θ is a feed-back input vector representing the joint orientation, $M(\theta)$ is a symmetric inertia matrix, which is positive definite for all $\theta \in R^2$ and $C(\theta,\dot{\theta})\dot{\theta}$ accounts for centrifugal and Coriolis torques. The term $F_v\dot{\theta}$ accounts for the friction torques vector and F_v accounts for the viscous friction. The Coulomb friction is compensated in the input torque τ. The effect of centrifugal force becomes evident on the distributed mass of the body. The term $C(\theta,\dot{\theta})$ is effective when the mass centre begins to move away from the centre of rotation. The centre of PTP is located on the rotational axis of the body and effect of term $C(\theta,\dot{\theta})$ is minimized. The term $g(\theta)$ accounts for the gravitational torque vector. The friction values were identified and presented in Section III. They have been determined experimentally and are modeled as:

$$F(\dot{\theta}) = F_v\dot{\theta} + F_c sgn(\dot{\theta}) \quad (2)$$

The nonlinearity lies in the $sgn(\dot{\theta})$; the output of the nonlinearity at any instant is determined by its input at that instant. Here F_v is Viscous friction and F_c *is* Coulomb friction. For a robot with 2-links such as PTP in Fig. 1 the nonlinear model using (1) and (2) is as:

$$\tau - F_c sgn(\dot{\theta}) = M(\theta)\ddot{\theta} + C(\theta,\dot{\theta})\dot{\theta} + F_v\dot{\theta} + g(\theta) \quad (3)$$

Here u = $\tau - F_c sgn(\dot{\theta})$ is a two dimensional control input. The nonlinear model of PTP is solved to obtain the state space model of the PTP below

$$\ddot{\theta} = -M^{-1}(\theta)\left[C(\theta,\dot{\theta}) + F_v\right]\dot{\theta} - M^{-1}(\theta)g(\theta) + M^{-1}(\theta)u \quad (4)$$

The state variables are x_1= Orientation of joint 1, x_2 = Angular velocity of joint 1, x_3 = Orientation of Joint 2, x_4= Angular velocity of joint 2. The state variables x_1, x_2, x_3, x_4 are variables whose values changes with time, they depend on the externally imposed values of input variables. The output variable value depends on the values of the state variables. Based on this, chosen the following state vectors x_a and x_b. Here

$$x_a = \begin{bmatrix} x_1 \\ x_3 \end{bmatrix} \text{ and } x_b = \begin{bmatrix} x_2 \\ x_4 \end{bmatrix} \quad (5)$$

The x_a is a state vector representing orientation of pan and tilt joints and x_b is a state vector for angular velocity for both the joints of PTP.

$$x_a = \theta, x_b = \dot{\theta} \quad (6)$$

Taking derivative of both sides

$$\dot{x}_a = \dot{\theta}, \dot{x}_b = \ddot{\theta} \quad (7)$$

Then the state space model is

$$\dot{x}_a = x_b \quad (8)$$

$$\dot{x}_b = -M^{-1}(x_a)[C(x_a, x_b) + F_v]x_b - M^{-1}(x_a)g(x_a) + M^{-1}(x_a)u \quad (9)$$

$$y = x_a \quad (10)$$

We have used the detailed model and accurate system parameters obtained through experiments and CAD. We have identified the system parameters; such as mass, inertia, and coriolis forces in Section III. Using the nonlinear state space model of the PTP in (8)-(10); the Simulink model of the PTP is presented in Fig. 3.

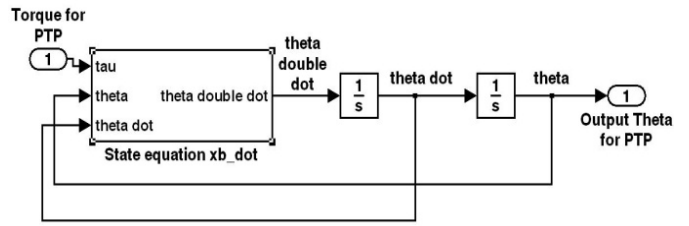

Fig. 3 Nonlinear model of the PTP

There are unknown parameters in the nonlinear state space model. We had found these experimentally or identified in CAD as in Section III.

3 Identification of Parameters

The unknowns in the state space model of the PTP are $F, C(\theta, \dot{\theta})$ and $M(\theta)$. The friction force F is composed of viscous friction F_v and Coulumb friction F_c. The F_v is a property of the medium in which the motion of the object is occurring. Here F_v in (9) is a frictional force that resists objects in motion. The viscous friction has been determined experimentally. The values of viscous friction are presented in Table I. The maximum value of frictions are taken from Table I [12], [13].

TABLE I
Viscous Friction

	Positive	Negative
F_v (pan) (Nms/rad)	0.0019	-0.0017
F_v (tilt) (Nms/rad)	0.0045	-0.0055

The nonlinear term in (3) is $F_c sgn(\dot{\theta})$. It is a force that exists between two objects that are in contact. The bodies act to prevent the motion of the objects. To complete an accurate non-linear model of the PTP, the Coulomb friction values were identified. The Coulomb friction exists between all moving parts in the system, such as the hinge and the bearings, the belts and the gears. The Coulomb friction values have been determined experimentally as in Table II.

TABLE II
Coulomb Friction

	Positive	Negative
F_c (tilt) (Nm)	0.0500	-0.0550
F_c(pan) (Nm)	0.0400	-0.0405

The required parameters in equation (9), masses and arm lengths were identified from CAD and they are summarized in Table III.

TABLE III
Arm Length and Mass

	Arm length (m)	Mass (Kg)
Pan mechanism	0.050	1.1452
Tilt mechanism	0.050	0.7395
PTP	-	1.8847

The pan mechanism in Fig. 1 is identical with uniform mass distribution, radius R_p, length l_p and mass m_p. The tilt mechanism is all identical with uniform mass distribution, height h_t, depth d_t, width w_t, and mass m_t. On the basis of these known parameters, (9) for PTP is as:

- Known parameters for pan mechanism: radius R_p, length l_p and mass m_p.
- Known parameters for tilt mechanism: height h_t, depth d_t, width w_t, and mass m_t.

The attributes of the PTP are defined using Euler rotation angle [1], here summarized as follows.

$$x = \begin{bmatrix}1\\0\\0\end{bmatrix}, y = \begin{bmatrix}0\\1\\0\end{bmatrix}, z = \begin{bmatrix}0\\0\\1\end{bmatrix} \text{ and } h_1 = z, h_2 = x$$

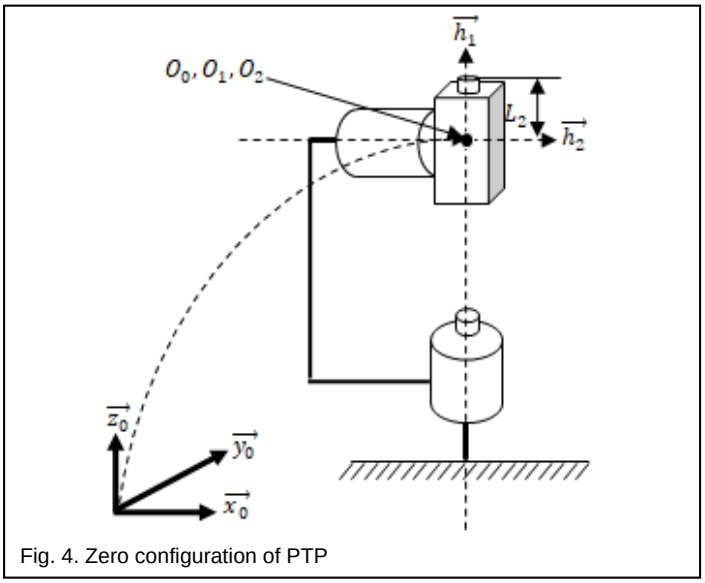

Fig. 4. Zero configuration of PTP

The position vector corresponding to both mechanisms and camera (end-effecter) is given as follows

$${}^0P_1 = {}^1P_2 = 0, \; {}^2P_E = L_2 z$$

Here ${}^0P_1$, ${}^1P_2$ and ${}^2P_E$ are the positions vectors belong to pan mechanism, tilt mechanism and camera respectively and ${}^0P_1$ indicates the position vector for pan mechanism with respect to ground frame. Similarly, ${}^1P_2$ indicates the position vector for tilt mechanism with respect to pan mechanism and ${}^2P_E$ with respect to tilt mechanism. By using definition of rotation matrix from [1], a rotation about the z and x axes can be represented by the following rotation matrices ${}^0R_1$ and ${}^1R_2$.

$$ {}^0R_1 = e^{\hat{\imath}_1\theta_1},\ {}^1R_2 = e^{\hat{\imath}_2\theta_2} \tag{11} $$

$$ {}^0R_1 = \begin{bmatrix} \cos\theta_1 & -\sin\theta_1 & 0 \\ \sin\theta_1 & \cos\theta_1 & 0 \\ 0 & 0 & 1 \end{bmatrix} \tag{12} $$

$$ {}^1R_2 = \begin{bmatrix} 1 & 0 & 0 \\ 0 & \cos\theta_2 & -\sin\theta_2 \\ 0 & \sin\theta_2 & \cos\theta_2 \end{bmatrix} \tag{13} $$

The Jacobian at each joint of PTP is found using the reference [1]. The Jacobian of pan joint J_1 is as follows.

$$ J_1 = \begin{bmatrix} z & 0 \\ 0 & 0 \end{bmatrix} \tag{14} $$

and Jacobian of tilt mechanism J_2 is as follows

$$ J_2 = \begin{bmatrix} {}^1R_2 z & x \\ \widehat{{}^2R_1 z}\ {}^2R_1\ {}^1P_2 & 0 \end{bmatrix} \tag{15} $$

The center of mass p_n^c for each body is found in (16), (17):

$$ p_1^c = -\left(\frac{l_p}{2}\right) z \tag{16} $$

$$ p_2^c = -\left(\frac{l_t}{2}\right) x \tag{17} $$

n indicates the pan and tilt mechanism n=1,2. The inertia of each body is found in (18)-(20) using [18]. The inertia matrix I_1^c for the pan mechanism is:

$$ I_1^c = \begin{bmatrix} \frac{m_p}{12}\left(3R_p^2 + l_p^2\right) & 0 & 0 \\ 0 & \frac{m_p}{12}\left(3R_p^2 + l_p^2\right) & 0 \\ 0 & 0 & \frac{m_p}{2}\left(R_p^2\right) \end{bmatrix} \tag{18} $$

The inertia matrix I_2^c for the tilt mechanism is:

$$ I_2^c = \begin{bmatrix} \frac{m_t}{12}({h_t}^2 + {w_t}^2) & 0 & 0 \\ 0 & \frac{m_t}{12}({h_t}^2 + {w_t}^2) & 0 \\ 0 & 0 & \frac{m_t}{12}({d_t}^2 + {w_t}^2) \end{bmatrix} \tag{19} $$

The inertia matrix I_E^c for the camera is:

$$ I_E^c = \begin{bmatrix} \frac{m}{12}({h_E}^2 + {w_E}^2) & 0 & 0 \\ 0 & \frac{m}{12}({h_E}^2 + {w_E}^2) & 0 \\ 0 & 0 & \frac{m}{12}({d_E}^2 + {w_E}^2) \end{bmatrix} \tag{20} $$

The $M(\theta)$, a symmetric inertia matrix, which is positive definite for all $\theta \in R^2$, is found using the following equations as follows.

$$ M_1 = \begin{bmatrix} I_1 & m_1\hat{P}_1^c \\ -m_1\hat{P}_1^c & m_1 I_1 \end{bmatrix} \tag{21} $$

$$ M_2 = \begin{bmatrix} I_2 & m_2\hat{P}_2^c \\ -m_2\hat{P}_2^c & m_2 I_2 \end{bmatrix} \tag{22} $$

$$ M_E = \begin{bmatrix} I_E & m_E\hat{P}_E^c \\ -m_E\hat{P}_E^c & m_E I_E \end{bmatrix} \tag{23} $$

$$ M(\theta) = \sum_{i=1}^{2} J_i^T M_i J_i \tag{24} $$

Here M_1, M_2 and M_E are the symmetric inertia matrices for pan, tilt mechanisms and camera. The kinetic energy of the PTP is:

$$ T = \frac{1}{2}\dot{\theta}^T M \dot{\theta} \tag{25} $$

To determine the effects of Coriolis and centrifugal forces the following equation is used from [2]

$$ C = \dot{M}(\theta, \dot{\theta}) - \frac{1}{2}\begin{bmatrix} \dot{\theta}^T \frac{\partial M}{\partial \theta_1} \\ \dot{\theta}^T \frac{\partial M}{\partial \theta_2} \end{bmatrix} \tag{26} $$

The potential energy of the pan P_1, tilt P_2 mechanisms are determined and presented as follows.

$$ P_1 = m_1\vec{g}.\left({}^0\vec{p}_1 + \vec{p}_1^c\right) \tag{27} $$

$$ P_2 = m_2\vec{g}.\left({}^0\vec{p}_1 + {}^1\vec{p}_2 + \vec{p}_2^c\right) \tag{28} $$

The total potential energy of the PTP is:

$$ P = P_1 + P_2 \tag{29} $$

The equations (11) to (29) are combined together to get the equation of motion as follows.

$$ \tau = M(\theta)\ddot{\theta} + C\left(\theta, \dot{\theta}\right)\dot{\theta} + g(\theta) \tag{30} $$

Here the matrices $M(\theta)$, $C\left(\theta, \dot{\theta}\right)$ and $g(\theta)$ are as follows:

$$ M = \begin{bmatrix} M_{11} & 0 \\ 0 & M_{22} \end{bmatrix} $$

$$ g(\theta) = \begin{bmatrix} 0 \\ 0 \end{bmatrix} $$

$$C(\theta,\dot{\theta}) = \begin{bmatrix} \frac{1}{6}\cos\theta_2 \sin\theta_2(-m_E d_E^2 - m_t d_t^2 + m_t h_t^2 + m_E h_E^2)\,\dot{\theta}_1\dot{\theta}_2 \\ -\frac{1}{12}\cos\theta_2 \sin\theta_2(-m_E d_E^2 - m_t d_t^2 + m_t h_t^2 + m_E h_E^2)\,\dot{\theta}_1^2 \end{bmatrix}$$

The terms M_{11} and M_{22} are found and given as:

$$M_{11} = \frac{1}{12}(\cos\theta_1)^2 m_E d_E^2 + \frac{1}{12}(\cos\theta_2)^2 m_t d_t^2 + \frac{1}{2}m_p R_p^2 + \frac{1}{12}m_t(h_t^2 + w_t^2) + \frac{1}{12}m_E w_E^2 + m_E L_2^2 + \frac{1}{4}m_t h_t^2 + \frac{1}{12}m_E h_E^2 - \frac{1}{12}(\cos\theta_2)^2 m_t h_t^2 - \frac{1}{12}(\cos\theta_2)^2 m_E h_E^2$$

$$M_{22} = \frac{1}{12}m_t h_t^2 + \frac{1}{12}m_t w_t^2 + \frac{1}{12}m_E(h_E^2 + w_E^2)$$

θ_n belongs to pan and tilt mechanisms respectively. The unknowns in the state space model are identified. The identified parameters $M(\theta)$, $C(\theta,\dot{\theta})$, F_v and centre of mass are used in MATLAB and Simulink simulation as in Section V. The centre of PTP is located on the rotational axis of the body and effect of term $C(\theta,\dot{\theta})$ is minimized. Therefore its effect is negligible. As the PTP of Fig. 1 the pan and tilt mechanisms are revolving about pan and tilt axis. Both the mechanisms are designed such that effect of g is minimized, due to the torque balancing.

4 Stability Analysis

The stability analysis of the PTP based on its equilibrium points is performed in this section. For the above state-space equation (8-9) of the PTP, we have found all the equilibrium points by putting $u = 0, \dot{x}_a = 0$ and $\dot{x}_b = 0$ as follows [2]

$$0 = x_b$$
$$0 = -M^{-1}(x_a)[C(x_a, x_b) + F_v]x_b - M^{-1}(x_a)g(x_a)$$

The equilibrium points are located at the $(x_1, 0, x_3, 0)$ where x_1 belongs to the set of real numbers from -2π to 2π and x_3 belongs to the set of real numbers from 0 to π/2. The function f(x) for the stability analysis of the tilt mechanism follows from (8-9). The type of each isolated equilibrium point can be found using the following function

$$f(x) = \begin{bmatrix} \dot{x}_a \\ \dot{x}_b \end{bmatrix} = \begin{bmatrix} x_b \\ -M^{-1}(x_a)[C(x_a, x_b) + F_v]x_b - M^{-1}(x_a)g(x_a) \end{bmatrix} \quad (31)$$

The centre of PTP is located on the rotational axis of the body and effect of term $C(\theta,\dot{\theta})$ is minimized and $M^{-1}(x_a) = M^{-1}$ because it is not effected by states. The effect of gravity is negligible. The behavior of the PTP can be analyzed using (31). The Jacobian of the tilt mechanism given below follows from (31).

$$\frac{\partial f}{\partial x} = \begin{bmatrix} 0 & 1 \\ 0 & -M^{-1}F_v \end{bmatrix} \quad (32)$$

The Jacobian of the tilt mechanism evaluated at $(x_1, 0, x_3, 0)$ is given below

$$A = \frac{\partial f}{\partial x}\Big|_{(x_1,0,x_3,0)} = \begin{bmatrix} 0 & 1 \\ 0 & -M^{-1}F_v \end{bmatrix} \quad (33)$$

The eigenvalues corresponding to the Jacobian determined were found as follows

$$|\lambda I - A| = \begin{vmatrix} \lambda & -1 \\ 0 & \lambda + M^{-1}F_v \end{vmatrix} \quad (34)$$

$$|\lambda I - A| = \lambda^2 + M^{-1}F_v\lambda = 0 \quad (35)$$

All the trajectories coverage to the equilibrium subspace as the $\lambda_2 < 0$ and $\lambda_1 = 0$ for pan mechanism and similarly for tilt mechanism. Thus PTP is marginally stable. The nonlinear control of the PTP is presented in next section.

5 LE model with PD controller

For the LE model of the PTP problem is to design the control law such that the required actuator inputs to the PTP are sufficient to perform the desired task, e.g. follow a desired input/ trajectory. The main objective of control system is to obtain the fastest time response with small overshoot and a smooth output signal enclosing small steady state error; for the desired input angles (θ_{pan}, θ_{tilt}).

The state space model (8-10) of the PTP is now evaluated using parameters identified in section III. The LE model of the PTP with the PD controllers is presented in figure 5. The subsystem block name nonlinear mathematical model of the PTP was controlled by the PD controllers.

The values obtained experimentally and available in CAD are presented in table I, II and III. These values are used in state space model of PTP in figure 5.

As shown in figure 5, the simulation consists of desired input angles, the PD controllers for pan and tilt mechanism, the PTP nonlinear model, actual output angles, and a quantizer in the feedback path. The quantization interval has been set to match the encoder resolution of 2π/4096. The zero-order hold (ZOH) block samples and holds its input for the specified sample period. The input of ZOH block is a vector; all elements of the vector are held for the same sample period.

The linearization simplifies the PTP model by focusing on each angle (θ_{pan}, θ_{tilt}) independently, for the pan and tilt mechanism. This LE model of PTP was linearized in order to develop a controller for the pan and tilt mechanisms in the [12]. The control law is as follows. [7], [8],[9],[10],[11]

$$KG_c = K(K_P e + K_D \dot{e}) \quad (36)$$

Here K, K_P and K_D are the gains and their values are presented in table IV.

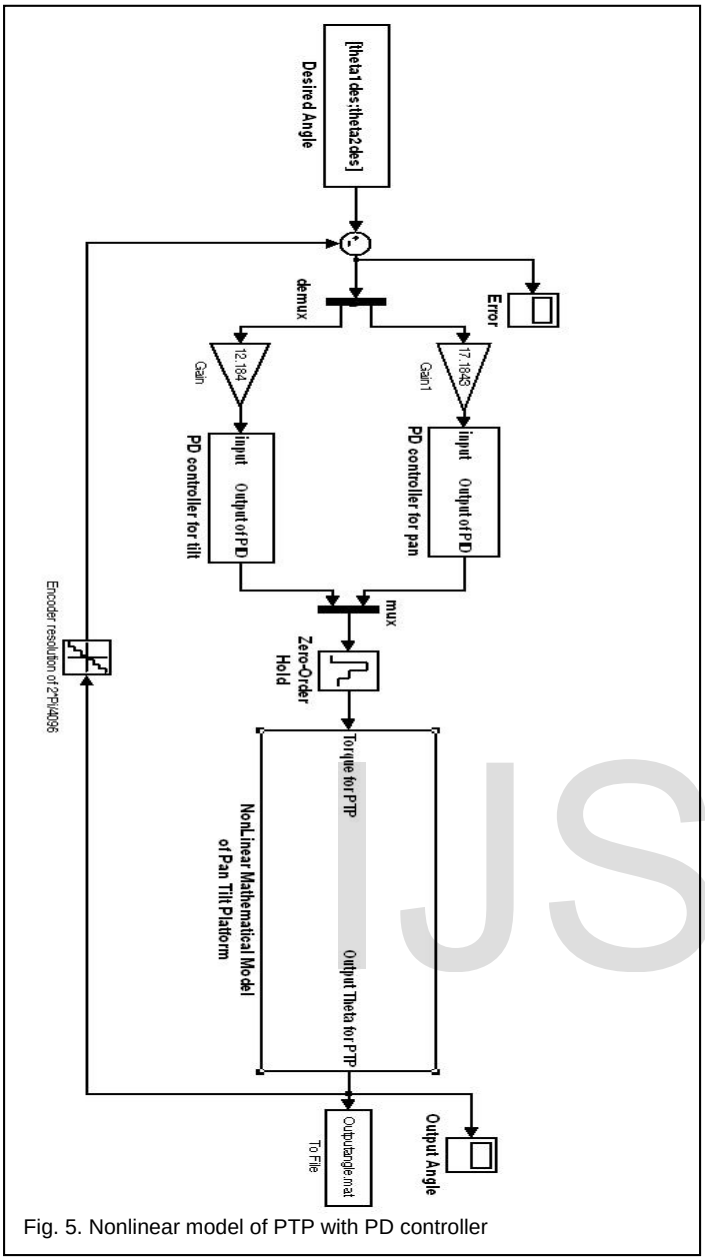

Fig. 5. Nonlinear model of PTP with PD controller

Table IV
The PD Controllers Gains

Gains	Pan Mechanism	Tilt Mechanism
K	17.1843	12.184
K_D	1	1
K_P	21.00	21.08

The result of input tracking system such as PTP with PD controllers is shown in figure 6. The angle achieved by pan and tilt mechanism are presented in figure 6 along with time.

The PD controllers worked with the same gains as found in [12] for the PTP in the presence of nonlinearities. As noticed in figure 6(a), for the tilt mechanism the setting time (0.1908 sec) and the steady-state error (1.9467×10-3) meet the desired performance values. Similarly in figure 6(b), for the pan mechanism the setting time (0.1905 sec) and the steady-state error (4.9881×10-3) meet the desired performance values.

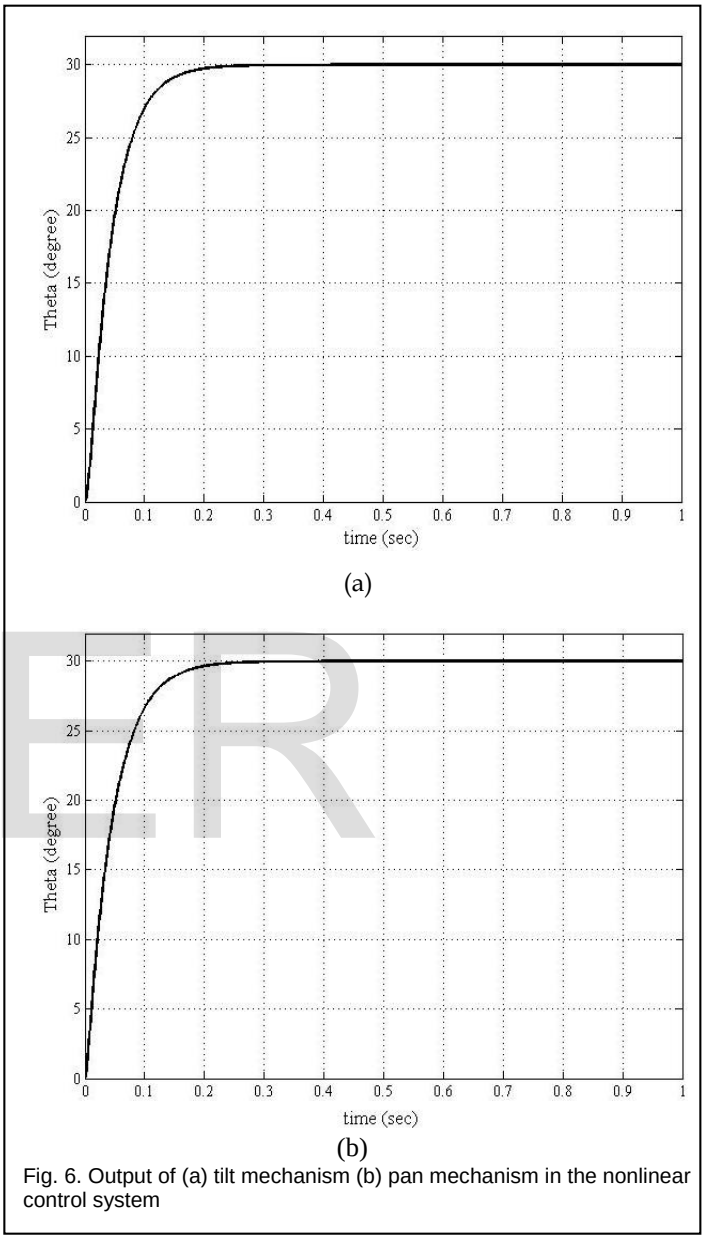

Fig. 6. Output of (a) tilt mechanism (b) pan mechanism in the nonlinear control system

6 Virtual Reality

In case of lengthy processes in design with fabrication the time span for the optimal solution is increased. This is reduced by using the simulation method. The benefit of such a simulation is that the solution cost and time are reduced. The basic aim of simulator is that to test the system with virtual environment created near to actual conditions. In virtual simulation gravity, backlash, dead zone, Coulomb friction, viscous friction and inertia effects were applied. [14]

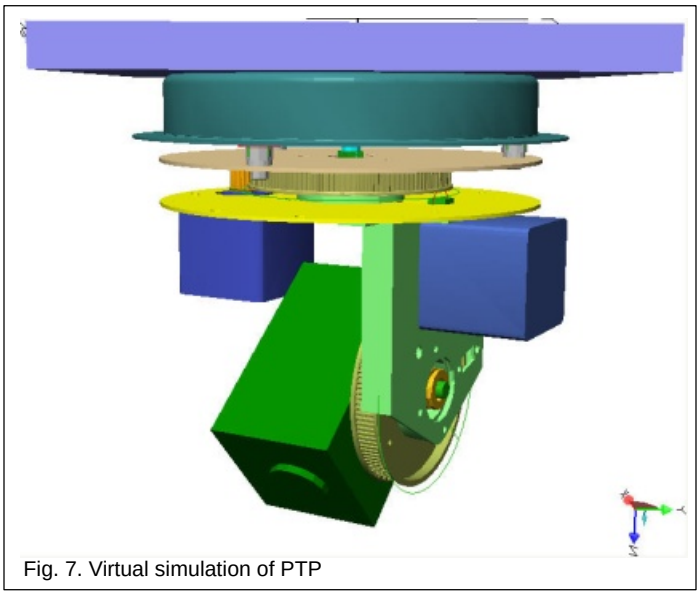

Fig. 7. Virtual simulation of PTP

The concept of virtual design of the PTP is to simulate virtual reality of the PTP that enabled us to interact with the design object in a three-dimensional virtual environment such as in MSC. VisualNastran-4D. The purpose of this research work is to construct a three-dimensional virtual design and simulation environment for the PTP. For this purpose structure of the PTP was modeled using Pro-E. The Pro-E model was transferred to dynamic simulation software for dynamical simulation with all mass and inertia properties. The fraction effect on each joint was applied using table I and II. In this environment, we can observe and interact with the design object exactly the same way as they observe and interact with real objects.

The controlled simulation was performed using Simulink and MSC.VisualNastran-4D of PTP as shown in figure 7. The use of Simulink in this work is to control the dynamics of a PTP using PD controller as shown in figure 8 for required orientation of the camera as shown in figure 7.

The aim of simulation is to test the system in virtual environment created as near to actual conditions. The fraction, gravity, backlash and dead zone effects were applied on the PTP. The effective value of the Coulomb friction, the viscous friction and gravity effects were applied in the MSC.VisualNastran-4D model. The process is explained by MSC.VisualNastran-4D model and Simulink control diagram in figure 7 and figure 8 respectively.

The PD controllers were applied as shown in figure 8. For the pan and tilt mechanisms the PD controller gains are given in table IV. The effect of nonlinearities upon the time response of the PTP is found in this virtual simulation. The nonlinearities inserted in Simulink model are saturation, dead zone and backlash as in figure 8.

The electronic amplifier is linear over a specific range but exhibits the nonlinearity called saturation at higher input voltages. The saturation limits were applied equal to ± 35 Nmm. The effect of saturation is to limit the torque applied by motor on the system. Without applying the saturation limit in virtual simulation system behavior is unpredictable as torque grows to very large value.

A DC motor that does not respond to very low input voltages due to frictional forces exhibits a nonlinearity called dead zone. The effect of dead zone is applied due to presence of the DC motor and gears assembly. The gears exhibit backlash [15], which occurs because of the loose fittings between two meshed gears. The mathematical model of backlash developed by [16] gives the trend of the backlash.

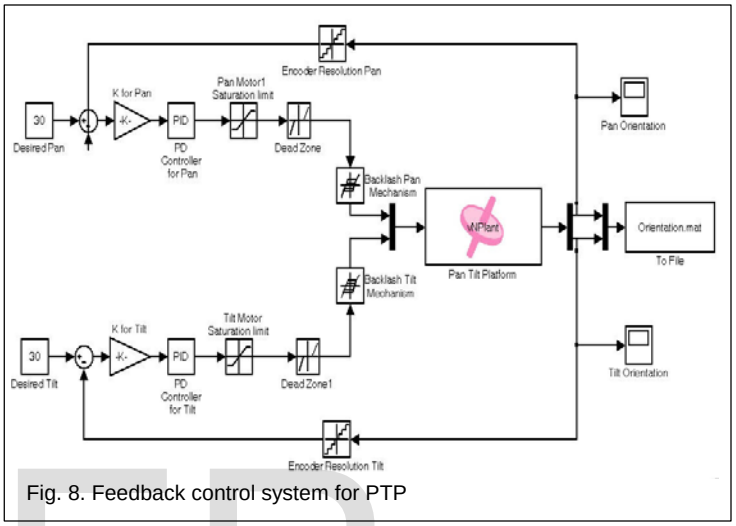

Fig. 8. Feedback control system for PTP

The result of virtual simulation for given inputs (θ_{pan}, θ_{tilt}) along with time is shown in figure 9.

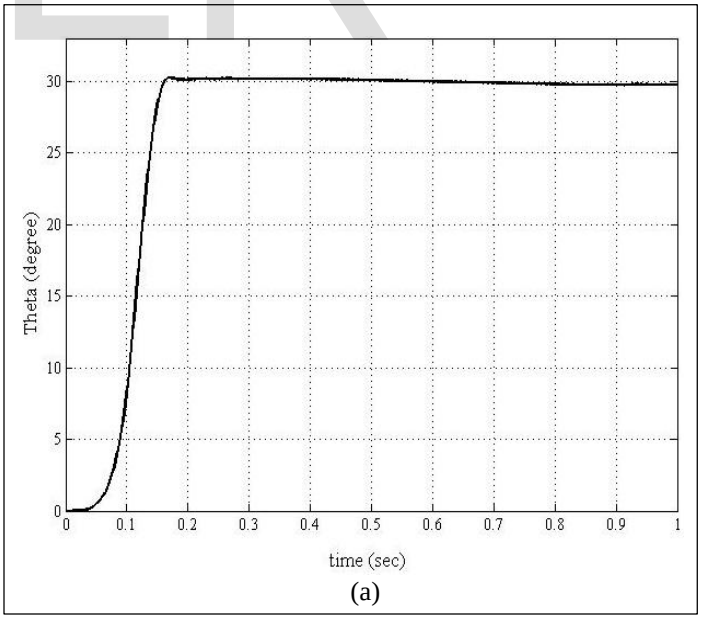

(a)

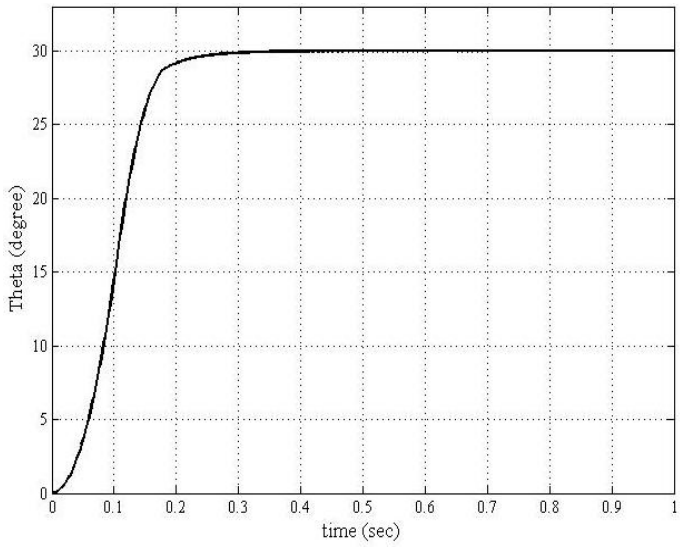

(b)

Fig. 9. Orientation of (a) tilt mechanism (b) pan mechanism in the virtual simulation environment

As noticed in figure 9(a), for the tilt mechanism the setting time (0.16 sec) and the steady-state error (4.4367×10^{-3}) meet the desired performance values. Similarly in figure 9(b), for the pan mechanism the setting time (0.21 sec) and the steady-state error (7.9351×10^{-3}) meet the desired performance values.

7 Results

The comparison of the LE model of the PTP controlled by the PD controllers and VisualNastran-4D model of PTP controlled by the PD controllers is presented in table V.

Table V
Models of PTP with PD controllers

	LE model with PD Controller		Virtual Simulation Controlled by PD Controller	
	T_S (seconds)	e_{ss}	T_S (seconds)	e_{ss}
Tilt Mechanism	0.1908	1.9467×10^{-3}	0.16	4.4367×10^{-3}
Pan Mechanism	0.1905	4.9881×10^{-3}	0.21	7.9351×10^{-3}

The result of LE model with PD controller and virtual simulation (CAD based technique) are matching closely with slight difference in the performance parameters. The difference in performance parameters are due to the backlash, saturation and dead zone, they are present in the CAD based technique. Thus, simulation results meet the desired performance values set according to movement of eye ball, such as settling time of eye ball, which is approximately 0.18~0.22 seconds.

The virtual simulation tool discussed and demonstrated material in this paper proves the efficacy of this tool and authenticates the results obtained from mathematical modelling based on LE equation.

The PD controller designed in [12] and used here works on nonlinear models because PTP operates under positioning control, the velocities are small.

8 Implementation

The design of a PTP is intended to perform a object tracking task mounted on a vehicle such as under unmanned aerial vehicles. The function of motion controllers is to track the desired inputs such that PTP points in desired direction. Based on initial position and output angles from motion controllers, the forward kinematics finds out final position (x, y, z) of camera and these coordinates x, *y, z* are compared with desired coordinates in image processing unit (IPU) and Laser range finder (LRF). The image grabber grabs the image from the camera mounted on the PTP and sends it into IPU. The IPU with LRF finds the desired *x, y, z* coordinates of the target. The coordinates are then sent into direct calculation / inverse kinematics unit and it converts these coordinates into desired input angles which are the inputs of motion controller shown in schematic figure 10.

In fig. 10, the input angles come from image processing unit and it takes output of digital camera as input. The 8051 microcontroller has been used as interface between image processing unit and LM628. The assembly code was developed and hex file was written in the flash memory of 80C51. The detail of algorithm and circuit is presented in [12]. The zero configuration of PTP is shown in figure 4.

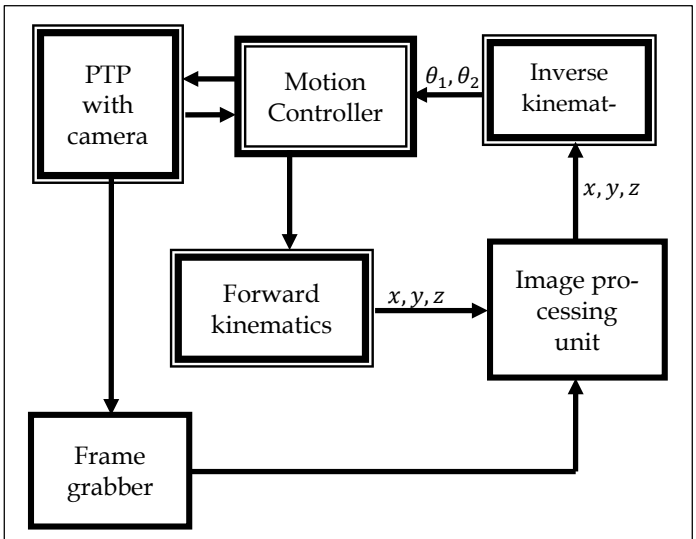

Fig. 10. Block diagram of PTP with motion controller and connected with image processing unit based on calculation carried out in kinematics blocks

The rotation matrix for pan, tilt and PTP are as follows.

$$ {}^{0}R_{1} = \begin{bmatrix} \cos\theta_1 & -\sin\theta_1 & 0 \\ \sin\theta_1 & \cos\theta_1 & 0 \\ 0 & 0 & 1 \end{bmatrix}, \quad (37) $$

$$ {}^{1}R_{2} = \begin{bmatrix} 1 & 0 & 0 \\ 0 & \cos\theta_2 & -\sin\theta_2 \\ 0 & \sin\theta_2 & \cos\theta_2 \end{bmatrix} \quad (38) $$

$$ {}^{0}R_{E} = \begin{bmatrix} \cos\theta_1 & -\sin\theta_1\cos\theta_2 & \sin\theta_1\sin\theta_2 \\ \sin\theta_1 & \cos\theta_1\cos\theta_2 & -\cos\theta_1\sin\theta_2 \\ 0 & \sin\theta_2 & \cos\theta_2 \end{bmatrix} \quad (39) $$

The position vector of PTP is given below.

$$ {}^{0}P_{E} = \begin{bmatrix} \sin\theta_1\sin\theta_2 \\ -\cos\theta_1\sin\theta_2 \\ \cos\theta_2 \end{bmatrix} L_2 \quad (40) $$

The forward kinematics is used to find the final pointing position of the camera. This is a 3 step process.

1. The initial position of the camera pointing is [x_0; y_0; z_0] = [0;0;1]. The next position [x_1; y_1; z_1] of the camera pointing is found using initial position and output angles achieved by motion controller.

$$ \begin{bmatrix} x_j \\ y_j \\ z_j \end{bmatrix} = \begin{bmatrix} \cos\theta_1 & -\sin\theta_1\cos\theta_2 & \sin\theta_1\sin\theta_2 \\ \sin\theta_1 & \cos\theta_1\cos\theta_2 & -\cos\theta_1\sin\theta_2 \\ 0 & \sin\theta_2 & \cos\theta_2 \end{bmatrix} \begin{bmatrix} x_{j-1} \\ y_{j-1} \\ z_{j-1} \end{bmatrix} \quad (41) $$

2. For next iteration j = 2, using the [x_{j-1}; y_{j-1}; z_{j-1}] = [x_1; y_1; z_1] as a previous position and new output angles achieved by motion controller in (41), the new pointing position [x_j; y_j; z_j] = [x_2; y_2; z_2]
3. Repeat step 2. For each new value of j=1,2,3,…..

The desired orientation of the PTP with a camera is defined by two angles are found on the basis of input from image processing unit in terms of x, y, z coordinates.

$$ \begin{bmatrix} \theta_1 \\ \theta_2 \end{bmatrix} = \begin{bmatrix} \arctan2(y, x) + 2\pi n \\ \arctan2(\sqrt{x^2 + y^2}, z) \end{bmatrix} \quad (42) $$

The desired orientation for the motion controller is found using the above equations. Consider a move from the point [x_0 y_0 z_0] = [10 0 10] on one side of the PTP to [x_1 y_1 z_1] = [−10 0 10] on the other side. The result from the above equation is a reference from [θ_1 θ_2] = [0° 45°] to [180° 45°]. Thus a rotation of 180° about pan axis is required to track the object.

9 Conclusion

This paper covers the PTP design based on kinematics, modeled with two different techniques. Then motion controllers are designed based on system dynamics. The performances of Langrage-Euler based mathematical model are compared with PTP dynamics simulation in the integrated dynamic simulation software's. This provides an accurate model of engineering systems such as electromechanical systems for performance and qualities evaluations. The model is a total torque, angle representation in three rigid body degrees of freedom in case of LE. These models are generalized, modularized and analytical representation of a PTP.

Acknowledgment

This work was supported by the Air University, the Pakistan Science Foundation and the Higher Education Commission of Pakistan.

References

[1] Craig J. J., "Introduction to Robotics Mechanics and Control", Addison-Wesley, 3rd edition, India, pp. 196-197, 2007.

[2] Khalil H. K., "Nonlinear System", Prentice Hall, 3rd edition, USA, pp. 19, 24, 2002.

[3] Anderson B. D. O.; Liu Y., "Controller reduction: Concepts and approaches", IEEE Trans. Automat. Contr., vol. 34, pp. 802-812, Aug 1989.

[4] Schilling R.J., "Fundamental of robotics analysis and control", Prentice Hall, USA, pp 60-70, 1990.

[5] Morris D. D.; Rehg J. M., "Singularity Analysis for Articulated Object Tracking", CVPR '98, Santa Barbara, CA, Jun 1998.

[6] Sarwar I. S., "Design, modeling and control of Pan Tilt Platform for unmanned aerial vehicle", M.S. thesis, Dept. Mechatronics Eng., NUST, Rawalpindi, Pakistan, 2006.

[7] Bennett S., "The Past of PID Controllers", Elsevier Science Ltd, Annual Reviews in Control 25, pp. 43-53, 2001.

[8] Rice B., Cooper D; "Design and Tuning of PID Controllers for Integrating (Non-Self Regulating) Processes", Proc. ISA 2002 Annual Meeting, Chicago, pp. 424-430, 2002.

[9] Reddy S. B., Garimella S. S., Srinivasan K. C., "Computer-aided design and analysis for a class of nonlinear systems", IEEE Contr. Syst. Mag., vol. 10, pp. 26-33, Jan 1990.

[10] Nise N. S., "Control Systems Engineering", Wiley student edition, Forth edition, pp. 514-531, 2004.

[11] Zhang J., Xu S., Li J., "A new design approach of PD controllers", Elsevier, pp. 329-336, Mar 2005.

[12] Sarwar I. S., Iqbal J., Malik A. M. "Modeling, analysis and motion control of a Pan Tilt Platform based on linear and nonlinear systems", in the Book "WSEAS Transactions on Systems and Control", Included in ISI/SCI Web of Science and Web of Knowledge, , Issue 8, Vol. 4, ISSN: 1991-8763, pp. 389–398, Aug 2009.

[13] Malabre M., "Some issues of structure and control for linear time-invariant systems", Elsevier Science Ltd, Annual Reviews in Control 30, 2006, pp. 131–141.

[14] Gebler D., Holtz J., "Identification and Compensation of Gear Backlash without Output Position Sensor in High-Precision Servo Systems", IECON '98. Proceedings of the 24th Annual Conference of the

IEEE, vol.2, pp. 662-666, Sep 1998.

[15] Nordin M., Galic J., Gutman P. O., "New models for backlash and gear play", Int. Journal of adaptive control and signal processing, vol.11, pp.49-63, 1997.

[16] Mohan M. A., "A new compensation technique for backlash in position control systems with elasticity", Proceedings of IEEE, 39th Southeastern symposium on system theory, pp. 244-248, Mar 2007.

[17] Paul R.C.P., "Robot manipulators: mathematics, programming and control", MIT, Press, Cambridge, pp. 68-75, 1981.

[18] Crowder R., "Electric drives and electromechanical systems", Elsevier, 1st edition, USA, pp. 38, 2006.

[19] Sinha R., Liang V., Paredis C J.J., Khosla P K., "Modeling and simulation methods for design of engineering systems", Journal of Computing and Information Science in Engineering, vol. 1, pp. 84-91, 2001